THE ASTROPHYSICAL JOURNAL, 358: L57–L61, 1990 August 1

NONLINEAR GROWTH OF RAYLEIGH-TAYLOR INSTABILITIES AND MIXING IN SN 1987A

IZUMI HACHISU AND TAKUYA MATSUDA
Department of Aeronautical Engineering, Kyoto University
AND
KEN'ICHI NOMOTO AND TOSHIKAZU SHIGEYAMA
Department of Astronomy, University of Tokyo
Received 1989 November 13; accepted 1990 May 11

ABSTRACT

Optical, X-ray, and gamma-ray light curves of SN 1987A and broad emission lines of heavy elements strongly suggest the occurrence of large-scale mixing during the explosion. Using a two-dimensional hydrodynamic code, we have numerically demonstrated a nonlinear growth of the Rayleigh-Taylor (R-T) instability in the ejecta of SN 1987A, which confirmed the linear stability analysis of Ebisuzaki, Shigeyama, and Nomoto and the two-dimensional hydrodynamical simulation of Arnett, Fryxell, and Müller 1989. After the blast shock breaks out of the helium core (~ 100 s after the explosion), a strong reverse shock forms behind the hydrogen/helium (H/He) interface and the R-T instability begins to largely grow at the H/He interface. Mushroom-like structures appear ~ 2000 s after the explosion. Eventually the core material (inside the carbon-oxygen layer) is mixed up to the layer having an expansion velocity of ~ 2200 km s^{-1} if the initial perturbation is as large as 5%. At the same time, hydrogen is mixed down to the core having an expansion velocity of ~ 800 km s^{-1}. The core material is concentrated into the high-density fingers with a density contrast of a factor of 5–6. Thus, the mixing due to the R-T instabilities can reproduce most of the observational indication of mixing in SN 1987A.

Subject headings: hydrodynamics — stars: individual (SN 1987A) — stars: supernovae

I. INTRODUCTION

Among the impacts from SN 1987A are the direct and indirect indications of large-scale mixing in the ejecta, which are summarized as follows:

1. Broad infrared emission lines of Fe II, Ni II, Ar II, and Co II (Erickson *et al.* 1988; Witteborn *et al.* 1989) and broad gamma-ray lines of ^{56}Co (Tueller *et al.* 1990) indicate the mixing of these heavy elements from the low-velocity core to the high-velocity outer envelope ($v = 2000$–3000 km s^{-1}).

2. Unexpectedly early emergences of hard X-rays (Dotani *et al.* 1987; Sunyaev *et al.* 1987) and gamma rays (Matz *et al.* 1988) are indirect evidences for mixing (e.g., Itoh *et al.* 1987; see Kumagai *et al.* 1989 for references). In order to reproduce the early gamma-ray light curve, it is necessary for a very small fraction of cobalt ($\sim 10^{-4}$ by weight) to be mixed up to the surface layer of $v \sim 3000$–4000 km s^{-1} (e.g., Kumagai *et al.* 1988, 1989; Pinto and Woosley 1988).

3. The smooth increase in the premaximum optical luminosity is well modeled by the radioactive decay heating of the photosphere around day ~ 25. This requires the mixing of ^{56}Ni to the layer having an expansion velocity of ~ 3000 km s^{-1} (Nomoto, Shigeyama, and Hashimoto 1987; Shigeyama, Nomoto, and Hashimoto 1988).

4. The plateau-like peak of the optical light curve is also well modeled by the presence of hydrogen-recombination front in the core. This is possible if hydrogen is mixed down to the metal-rich core where the expansion velocity is as low as 800 km s^{-1} (Shigeyama 1989; Shigeyama and Nomoto 1990; Nomoto *et al.* 1988). The minimum velocity of hydrogen has been actually found to be as low as ~ 800 km s^{-1} (Höflich 1988).

5. The very slow decline in the hard X-rays observed with *Ginga* (Tanaka 1988) requires the effective reduction of photoelectric absorption by heavy elements, which suggests the presence of chemically inhomogeneous clumps, in particular, hydrogen-helium–rich *hole* in the core (Kumagai *et al.* 1989). Such a clumpy structure is directly suggested from some spectral features (Stathakis, Dopita, and Canon 1989).

The most promising mechanism to mix the ejecta of SN 1987A is the Rayleigh-Taylor (R-T) instability (Chevalier 1976; Falk and Arnett 1977). The nonlinear growth of the instability for an explosion of a polytrope of index 3 was simulated by Nagasawa, Nakamura, and Miyama (1988) using a three-dimensional smoothed particle hydrodynamic code; they found strong convective instability and mixing in the ejected shell (also Nagasawa 1990). However, only a weak instability was found for the same polytrope by Müller *et al.* (1989) and Benz and Thielemann (1990*b*). The origin of the instability in this case may be related to how the shock wave is initiated (Nagasawa 1990) and is an active controversy.

The importance of the realistic presupernova density structure has been demonstrated in the linear stability analyses by Ebisuzaki, Shigeyama, and Nomoto (1989) and Benz and Thielemann (1990*a*) and for the nonlinear regime by Arnett, Fryxell, and Müller (1989, hereafter AFM). The linear analyses performed for the realistic model of SN 1987A, 14E1 (Shigeyama and Nomoto 1990), have shown that the hydrogen/helium (H/He) and helium/heavy element (He/C+O) interfaces are strongly R-T unstable. AFM have carried out two-dimensional axisymmetric hydrodynamical simulations for the 15 $M_\odot$ model of SN 1987A (Arnett 1987) and found a pronounced nonlinear growth of the R-T instability around the He/C+O interface. This is basically in agreement with the linear stability analyses.

In AFM, however, the instability around the H/He interface is not significant, which is different from the linear analysis.

This discrepancy may stem mainly from the difference in the initial models. Compared with model 14E1 which has a 6 $M_\odot$ helium core (Nomoto, Shigeyama, and Hashimoto 1987), Arnett's (1987) 15 $M_\odot$ model has a smaller helium core (4 $M_\odot$) that is more centrally concentrated; in particular, the density gradient is much steeper near the He/C+O interface. Moreover, AFM assumed that the neutron star mass is zero and a shock wave forms at the center of the progenitor. This assumption corresponds effectively to an enhanced postshock density gradient around the He/C+O interface if compared with the more realistic model that forms a shock wave at the iron core edge (Fig. 5 of Arnett 1988).

In view of the wide theoretical and observational importance to resolve these controversies, we have performed independently two-dimensional hydrodynamical calculations to clarify the question on the origin of the R-T instability. In our calculation presented in this *Letter*, we use an axisymmetric two-dimensional hydrodynamic code with 2–3 × 10^6 mesh points and adopt a progenitor model 14E1 as summarized in § II. We have basically confirmed the nonlinear growth of the R-T instability as found by AFM. There are some differences, however, from their result, i.e., the instability starts to grow not at the He/C+O interface but at the H/He interface. We have also examined the extent of mixing by using marker particles for quantitative comparison with the observations. These results are presented in § III and compared with the observations in § IV.

II. MODELS AND NUMERICAL CODE

Our progenitor model and the explosion parameters for SN 1987A are the same as model 14E1 (Nomoto *et al.* 1988; see Shigeyama and Nomoto 1990 for details). The progenitor had 21 $M_\odot$ on the main sequence and 16.3 $M_\odot$ at the explosion; its helium core mass is 6 $M_\odot$ (Saio, Nomoto, and Kato 1988). The final kinetic energy of explosion is 1×10^{51} ergs, and the ejecta has a mass of 14.7 $M_\odot$ with a 1.6 $M_\odot$ neutron star left behind.

The shock propagation through the middle of the hydrogen-rich envelope (up to $t = t_0$; t_0 = 140 or 1000 s) is calculated using a one-dimensional Lagrangian code with 700 meshes and dynamic rezoning (Shigeyama 1989; Shigeyama and Nomoto 1990). Then the density, velocity, energy etc. are interpolated and mapped onto our two-dimensional grids. Just after the mapping, we perturb only the velocity field all over the mesh points; i.e., the velocity field inside the shock front is perturbed, but the velocities outside the shock remain zero. Two types of perturbation are applied: (1) periodic sinusoidal perturbation, which is represented by $1 + \epsilon \cos(m\theta)$; and (2) random perturbation (we divide the latitudinal angle into N pieces and perturb randomly the velocity field at each π/N latitudinal angle; N = 32 or 128). The amplitude of the perturbation is 5%, i.e., $\epsilon = 0.05$ unless otherwise specified.

We solve the Euler equations with a constant adiabatic index $\gamma = 4/3$; this is a good approximation for the present radiation dominant situation. Our numerical method is the second-order Lax-Wendroff scheme with Davis's (1984) TVD (total variation diminishing) artificial viscosity. Davis's TVD artificial viscosity completely suppresses overshooting at the shock front and oscillations at the contact surface. This numerical scheme is easily vectorized and simple so that about 10^6 zones can be computed per second on a single Fujitsu VP-400E processor (~300 megaflops). Therefore, one case can be computed in 2 hr (1025 × 2049) or 5 hr (1793 × 1793) CPU time on a VP-400E.

TABLE 1

MAXIMUM AND MINIMUM VELOCITIES OF COMPOSITION INTERFACES

Number of Run	t_0 (s)	Mesh	$\Delta R = \Delta Z$ (10^9 cm)	Type of Perturbation[a]	V_{max}/V_{min} (km s^{-1})
1...........	140	1025 × 2049	0.96	$m = 10$	2500/1280[b]
2...........	140	1025 × 2049	0.96	$m = 20$	2410/1390[b]
3...........	140	1025 × 2049	0.96	Random (32)	2460/1360[b]
4...........	140	1793 × 1793	1.65	$m = 20$	2220/740[c]
5...........	1000	1793 × 1793	1.34	$m = 40$	2200/670[d]
6...........	1000	1793 × 1793	1.34	Random (128)	1880/620[d]

[a] $\epsilon = 0.05$.
[b] Velocity of He/C+O interface at $t \sim 3000$ s.
[c] Velocity of He/C+O interface at $t \sim 10{,}000$ s.
[d] Velocity of O/Si interface ($M_r = 0.15\ M_\odot$) at $t \sim 10{,}000$ s.

In order to accurately follow the growth of the R-T instability, we must calculate the shock propagation through the entire hydrogen-rich envelope of the star. Since the ratio of the radius between the hydrogen-rich envelope and the helium core is ~100 when the shock hits the envelope, more than 1000 mesh points per one dimension may be necessary.

In the present calculation, we use two types of mesh: one covers $\theta = 0 - \pi$ with 1025 × 2049 mesh points ($R \times Z$; equal mesh interval in a cylindrical coordinate system with $\Delta R = \Delta Z = 0.965 \times 10^9$ cm) and the other covers $\theta = 0 - \pi/2$ with 1793 × 1793 mesh points. In the latter case, we assume equatorial symmetry. These zone numbers are large enough to resolve the large-scale mushroom structures as will be seen later but still may not be enough to resolve small scale structures and mixing.

To examine the extent of mixing, we follow the positions of 3075 (or 12291) marker particles which are initially placed at the H/He ($M_r = 4.4\ M_\odot$), He/C+O ($M_r = 2.2\ M_\odot$), and oxygen/silicon (O/Si) ($M_r = 0.15\ M_\odot$) interfaces. The calculations are performed for several combinations of the initial time (t_0 = 140 and 1000 s), the mesh (1025 × 2049 and 1793 × 1793), and the type of perturbation (m = 10, 20, 40, and random perturbation). These are summarized in Table 1.

III. NUMERICAL RESULTS

a) *Early Development of Mushroom Structures*

Just after the blast shock hits the hydrogen-rich envelope (~100 s after the explosion), a strong reverse shock forms behind the H/He interface; then the R-T instability sets in at the H/He interface and continues to grow until the blast shock breaks out of the hydrogen-rich envelope. To see an early development of the R-T instability, we have started our computation at $t = t_0$ = 140 s (see runs 1–3 of Table 1). The growth time to nonlinear regime is about 1000 s and the mushroom structures become apparent at t = 2000 s. Figure 1 shows the density contour map at t = 3109 s for run 2. Each contour is linearly spaced by 5%. The spacing between two mushroom structures is almost equal and periodic.

The mushroom-like structures, which are manifestation of the R-T instability, depend on the type of the initial perturbation. In fact no mushroom structures appear if we introduce no perturbations. For run 2 in Figure 1, the number of mushroom structures is 10, which is closely related to the choice of m = 20. Applying other types of perturbation, we follow the

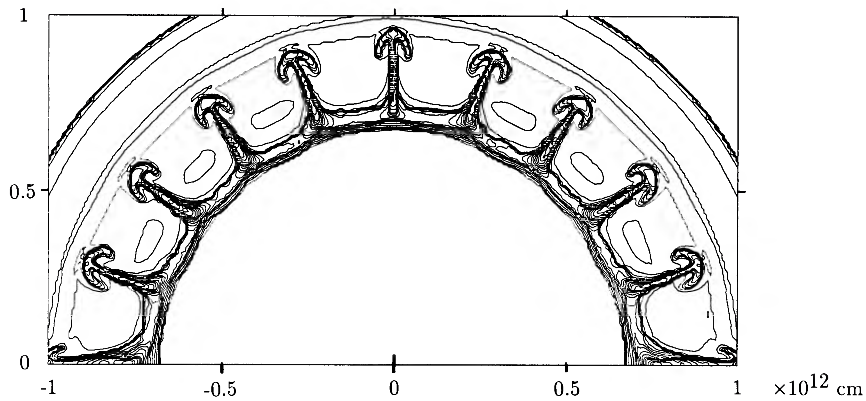

FIG. 1.—Density contour map at $t = 3109$ s after the explosion for run 2. Each contour is linearly spaced by 5%. The lowest bound is the rotation axis. The size of the computational region ($R \times Z$) is $1 \times 10^{12} \times 2 \times 10^{12}$ cm^2. A part of the blast shock front is seen in the upper right and upper left corner of the figure. The reverse shock is converging toward the center at this time but not seen in the figure because of the too low density in the central region. The locations of the H/He and He/C + O interfaces can be seen from the comparison with Fig. 3.

growth of the R-T instability using the same mesh points as above. For $m = 10$, the number of the mushroom structures is five and the growth of the instability is almost the same as for $m = 20$. For $m \gtrsim 40$, a much larger number of mesh points are needed to resolve such small-scale structures, which will be discussed in detail in a separate paper.

For a random perturbation with $N = 32$ (run 3), the density contour map at $t = 3285$ s is shown in Figure 2. (It should be noted that the contour resolutions in Figs. 1–3 are coarser than the actual calculations because only 129×257 mesh points were used in making plots.) Here the growth rate and the number of mushroom structures (~ 10) are both almost the same as found in the periodic case of $m = 20$. For a much finer random perturbation with $N = 128$ (run 6), the number of mushroom structures is larger, i.e., ~ 20 at the $\theta = 0 - \pi$ region. This implies that the mushroom structures are also dependent on the wave number N.

b) *Mixing*

The R-T instability, being initiated first at the H/He interface, induces the mixing between the core and the envelope. Figure 3 shows the positions of the marker particles at $t = 3109$ s for the case in Figure 1 (run 2). It is clear that the heavy elements (core material) are mixed up to the middle of the hydrogen-rich envelope. The extent of mixing can be represented by the maximum and minimum velocities of the He/C + O and O/Si interfaces. Using another mesh, we have followed further development of the R-T instability through $t \sim 10{,}000$ s, at which the velocities reach almost the terminal values (runs 4–6). The maximum and minimum velocities of the composition interfaces are summarized in Table 1.

Figure 4 shows the radial positions and the absolute velocities at $t \sim 10{,}000$ s of the marker particles initially situated at the H/He, He/C + O, and O/Si interfaces for run 5. The core materials composed of C + O and silicon-rich elements are mixed up to the layers having expansion velocities of ~ 2200 km s^{-1}. At the same time, hydrogen is mixed down to the core of expansion velocities as low as ~ 800 km s^{-1}. These velocities are close to the terminal values, since the shock has already broken out of the hydrogen-rich envelope at this time.

The abundance distributions after mixing as a function of mass are given in Nomoto *et al.* (1990) for the present calculations and in Müller, Fryxell, and Arnett (1990) for the update models of AFM. These two results are consistent with each

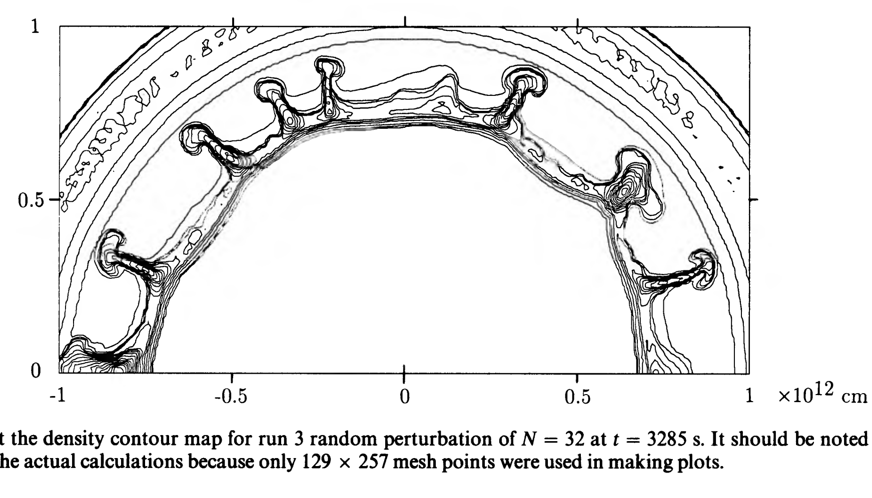

FIG. 2.—Same as Fig. 1 but the density contour map for run 3 random perturbation of $N = 32$ at $t = 3285$ s. It should be noted that the contour resolutions in Figs. 1 and 2 are coarser than the actual calculations because only 129×257 mesh points were used in making plots.

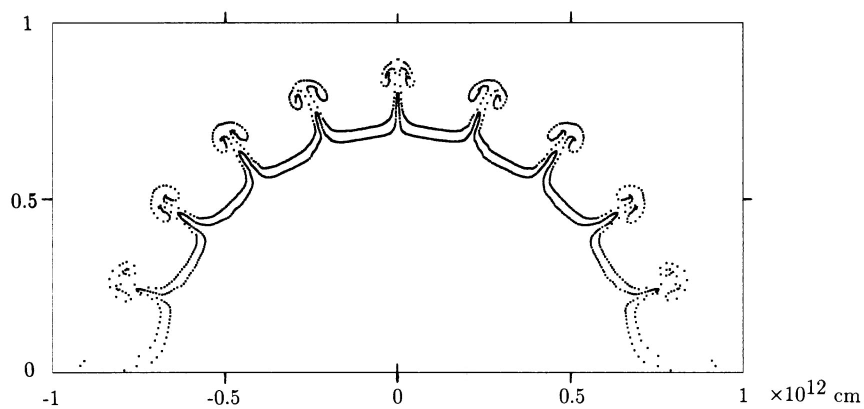

FIG. 3.—Positions of the marker particles at $t = 3109$ s for run 2. Inner side particles show the He/C+O interface, and the outer side particles correspond to the H/He interface. The core material finally reaches the top of the mushroom head at $t \sim 6000$ s.

other, although the interface from which the dominant instability starts to grow is different.

IV. DISCUSSION

Our results presented above are found to be basically consistent with AFM and should be compared with the observations. The calculated extent of the R-T mixing in velocity space can quantitatively account for most of the observational indications of the mixing as summarized in § I. As for the clumpy structures, heavy elements are concentrated into the high-density fingers so that the hydrogen-helium–rich fingers may effectively be *holes* for X-rays because of much smaller photoelectric absorption. Note also that dust may form preferentially in the high-density clumps, which can account for why the dust formed in the ejecta has not led to the blackout of the supernova (Lucy *et al.* 1989; Kozasa, Hasegawa, and Nomoto 1989).

Regarding the early emergence of gamma rays, which requires the mixing of trace ^{56}Ni up to the region with an expansion velocity of as large as $\sim$3000–4000 km s^{-1}, the R-T instability alone may not convey nickel to the very surface layer. In order to check the dependency of the mixing on the initial amplitude of perturbation, we have tried two other cases of $\epsilon = 0.01$ and 0.20. The 1% perturbation is too small to mix the ejecta. Even with the 20% perturbation, the maximum velocity of O/Si interface cannot exceed 2500 km s^{-1}. The starting time of two-dimensional calculation does not severely affect the mixing if $t_0 \lesssim 1000$ s. Further acceleration of the core material on a much longer time scale may be possible because of a later energy input by the decay of ^{56}Ni (Woosley, Pinto, and Ensman 1988; Arnett 1988). Alternatively, the effect of clumpiness on the gamma-ray emergence could be significant.

We would like to thank Dave Arnett for useful suggestions for improving the original manuscript. K. N. and T. M. are grateful to Ewald Müller, Wolfgang Hillebrandt, Dave Arnett, and Bruce Fryxell for fruitful discussion and hospitality during the visit to Garching and Tucson. The computation was carried out on a Fujitsu VP-400E vector processor of the Data Processing Center of Kyoto University. This work has been supported in part by the Grant-in-Aid for Scientific Research (01540216, 01652506, 01790169, 02234206, 02302024, 02640204) of the Japanese Ministry of Education, Science, and Culture, and by the Japan–US Cooperative Science Program (EPAR-071/88-15999) operated by the JSPS and the NSF.

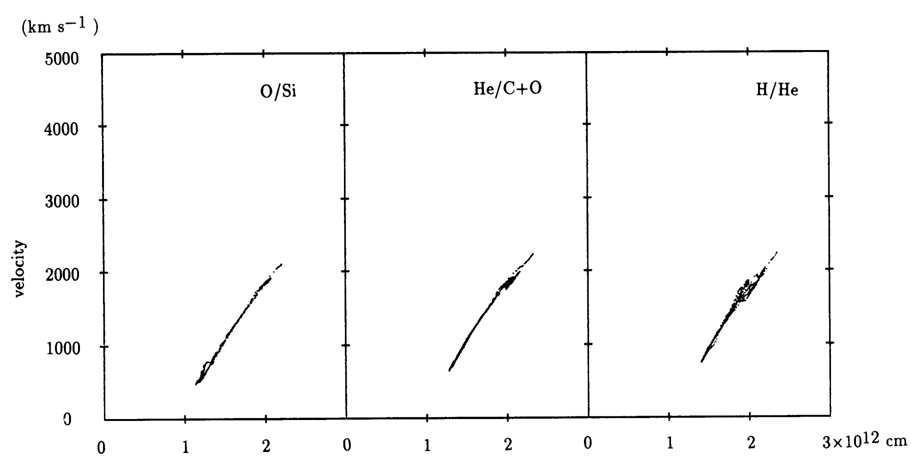

FIG. 4.—Velocity vs. radial position of the marker particles at $t = 9768$ s for run 5: (*right*) H/He interface, (*center*) He/C+O interface, and (*left*) O/Si interface. These velocities are almost terminal values, though the flow is still R-T unstable at this time and the maximum velocity is slightly changing.

REFERENCES

Arnett, W. D. 1987, *Ap. J.*, **319**, 136.
———. 1988, in *Supernova 1987A in the LMC*, ed. M. Kafatos and A. Michalitsianos (Cambridge: Cambridge University Press), p. 301.
Arnett, W. D., Fryxell, B. A., and Müller, E. 1989, *Ap. J. (Letters)*, **341**, L63 (AFM).
Benz, W., and Thielemann, F.-K. 1990*a*, *Ap. J. (Letters)*, **348**, L17.
———. 1990*b*, in *Supernovae*, ed. S. E. Woosley (Berlin: Springer-Verlag), in press.
Chevalier, R. A. 1976, *Ap. J.*, **207**, 872.
Davis, S. F. 1984, NASA Contractor Report 172373, ICASE REPORT No. 84-20.
Dotani, T., *et al.* 1987, *Nature*, **330**, 230.
Ebisuzaki, T., Shigeyama, T., and Nomoto, K. 1989, *Ap. J. (Letters)*, **344**, L65.
Erickson, E. F., Haas, M. R., Colgan, S. W. J., Lord, S. D., Burton, M. G., Wolf, J., Hollenbach, D. J., and Werner, M. 1988, *Ap. J. (Letters)*, **330**, L39.
Falk, S. W., and Arnett, W. D. 1977, *Ap. J. Suppl.*, **33**, 515.
Höflich, P. 1988, *Proc. Astr. Soc. Australia*, **7**, 434.
Itoh, M., Kumagai, S., Shigeyama, T., Nomoto, K., and Nishimura, J. 1987, *Nature*, **330**, 233.
Kozasa, T., Hasegawa, H., and Nomoto, K. 1989, *Ap. J.*, **344**, 325.
Kumagai, S., Itoh, M., Shigeyama, T., Nomoto, K., and Nishimura, J. 1988, *Astr. Ap.*, **197**, L7.
Kumagai, S., Shigeyama, T., Nomoto, K., Itoh, M., Nishimura, J., and Tsuruta, S. 1989, *Ap. J.*, **345**, 412.
Lucy, L. B., Danziger, I. J., Gouiffes, C., and Bouchet, P. 1989, in *IAU Colloquium 120, Structure and Dynamics of the Interstellar Medium*, ed. G. Tenorio-Tagle, M. Moles, and J. Melnick (Berlin: Springer-Verlag), in press.
Matz, S. M., Share, G. H., Leising, M. D., Chupp, E. L., Vestrand, W. T., Purcell, W. R., Strickman, M. S., and Reppin, C. 1988, *Nature*, **331**, 416.
Müller, E., Fryxell, B., and Arnett, W. D. 1990, in *Chemical and Dynamical Evolution of Galaxies*, ed. F. Ferrini, J. Franco, and F. Matteucci (Pisa: Giondini), in press.
Müller, E., Hillebrandt, W., Orio, M., Höflich, P., Mönchmeyer, R., and Fryxell, B. A. 1989, *Astr. Ap.*, **220**, 167.
Nagasawa, M. 1990, *Ap. J. (Letters)*, submitted.
Nagasawa, M., Nakamura, T., and Miyama, S. M. 1988, *Pub. Astr. Soc. Japan*, **40**, 691.
Nomoto, K., Shigeyama, T., Kumagai, S., and Hashimoto, M. 1988, *Proc. Astr. Soc. Australia*, **7**, 490.
Nomoto, K., Shigeyama, T., and Hashimoto, M. 1987, in *SN 1987A*, ed. I. J. Danziger (Garching: ESO), p. 325.
Nomoto, K., Hachisu, I., Matsuda, T., Hashimoto, M., Shigeyama, T., Kumagai, S., and Yamaoka, H. 1990, in *Chemical and Dynamical Evolution of Galaxies*, ed. F. Ferrini, J. Franco, and F. Matteucci (Pisa: Giondini), in press.
Pinto, P. A., and Woosley, S. E. 1988, *Ap. J.*, **329**, 820.
Saio, H., Nomoto, K., and Kato, M. 1988, *Nature*, **334**, 508.
Shigeyama, T. 1989, Ph.D. thesis, University of Tokyo.
Shigeyama, T., and Nomoto, K. 1990, *Ap. J.*, in press.
Shigeyama, T., Nomoto, K., and Hashimoto, M. 1988, *Astr. Ap.*, **196**, 141.
Stathakis, R. A., Dopita, M. A., and Cannon, R. D. 1989, preprint.
Sunyaev, R., *et al.* 1987, *Nature*, **330**, 227.
Tanaka, Y. 1988, in *Physics of Neutron Stars and Black Holes*, ed. Y. Tanaka (Tokyo: Universal Academy Press), p. 431.
Tueller, J., Barthelmy, S., Gehrels, N., Teegarden, B. J., Leventhal, M., and MacCallum, C. J. 1990, *Ap. J. (Letters)*, **351**, L41.
Witteborn, F. C., Bregman, J. D., Wooden, D. H., Pinto, P. A., Rank, D. M., Woosley, S. E., and Cohen, M. 1989, *Ap. J. (Letters)*, **338**, L9.
Woosley, S. E., Pinto, P. A., and Ensman, L. 1988, *Ap. J.*, **324**, 466.

Izumi Hachisu and Takuya Matsuda: Department of Aeronautical Engineering, Kyoto University, Kyoto 606, Japan

Ken'ichi Nomoto and Toshikazu Shigeyama: Department of Astronomy, Faculty of Science, University of Tokyo, Bunkyo-ku, Tokyo 113, Japan